



# Generation of 172 fs pulse from a Nd: YVO<sub>4</sub> picosecond laser by using multi-pass-cell technique

Jiajun Song<sup>1,2</sup> · Zhaohua Wang<sup>1,5</sup> · Renchong Lv<sup>3</sup> · Xianzhi Wang<sup>1,2</sup> · Hao Teng<sup>1</sup> · Jiangfeng Zhu<sup>3</sup> · Zhiyi Wei<sup>1,2,4</sup>

Received: 18 September 2020 / Accepted: 5 February 2021 / Published online: 17 March 2021  
© The Author(s), under exclusive licence to Springer-Verlag GmbH, DE part of Springer Nature 2021

## Abstract

The device of multi-pass-cell (MPC) could broaden the spectra of ultrafast laser pulses based on the self-phase-modulation (SPM) effect, which is composed of two concave mirrors and nonlinear mediums. In this paper, the pulse duration of 172 fs is compressed from a 11.3 ps Nd: YVO<sub>4</sub> regenerative amplifier at the repetition rate of 1 kHz by using two stages of MPC systems. The pulse duration is shortened by a factor of 66, and the pulse energy of 117 μJ is obtained with a total efficiency of 51%. With high average power Nd-doped laser systems at 10 ps level, this method has the potential to generate high power femtosecond lasers with high efficiency, compact configuration, and low cost.

## 1 Introduction

Ultrafast femtosecond laser systems with hundreds of microjoules energy operated at several kilohertz repetition rate are of great importance to many applications like medical science [1], industrial processes [2, 3], mid-infrared generation [4] and impulsive coherent vibrational spectroscopy [5, 6]. To boost the energy of the femtosecond oscillator to hundreds of microjoules or higher, the chirped pulse amplification (CPA) technology based on bulk gain mediums is generally applied. All kinds of costly dispersive elements like chirped mirrors, Gires-Tournois (GTI) mirrors, transmission/reflection gratings and chirped fiber Bragg grating (CFBG) are normally employed in CPA devices, which increases the

complexity and cost of the laser system [7–9]. However, the mode-locked Nd: YVO<sub>4</sub> oscillators can radiate 10 ps pulses without dispersive elements, which can be amplified to hundreds of microjoules or even several millijoules directly without CPA technology [10, 11]. In addition, combining with nonlinear spectral broadening and pulse compressing technologies, the 10 ps level ultrafast laser sources would become attractive devices for generating compact and cost-efficient femtosecond lasers.

Several nonlinear spectral broadening processes have been reported, such as cross-polarized wave generation (XPW), cascade second-order nonlinear effect and self-phase modulation (SPM). Limited by the conversion efficiency ( $\leq 33\%$  [12]) and the spectral broadening ratio ( $\leq 1.73$  [13]), XPW is seldomly used for spectral broadening [14]. The maximum pulse compression ratio based on the cascaded second-order nonlinearity is only 6.3 to date. To get this ratio, 3 stage BBO crystals were employed [15]. Compared to the above two principles, SPM has the advantages of a higher spectral broadening factor and less energy loss. Several kinds of devices have been demonstrated based on the SPM effect, such as the solid-core photonic crystal fiber (PCF) [16–18], the gas-filled Kagome hollow-core PCF [19–23], the noble gas-filled hollow-core capillaries (HCF) [24–30], the solid thin plates (STP) [31–33] and the MPC [34–43]. An overview of the reported input laser pulse parameters of different devices based on SPM effect is shown in Fig. 1. Limited by the self-focusing threshold of the glass material (a few MW), the solid core PCF is normally utilized for the spectral broadening of the femtosecond

✉ Zhaohua Wang  
zhwang@iphy.ac.cn  
Zhiyi Wei  
zywei@iphy.ac.cn

<sup>1</sup> Beijing National Laboratory for Condensed Matter Physics, Institute of Physics, Chinese Academy of Sciences, Beijing 100190, China

<sup>2</sup> School of Physical Sciences, University of Chinese Academy of Sciences, Beijing 100049, China

<sup>3</sup> School of Physics and Optoelectronics Engineering, Xidian University, Xi'an 710071, China

<sup>4</sup> Songshan Lake Materials Laboratory, Dongguan 523808, Guangdong, China

<sup>5</sup> CAS Center for Excellence in Ultra-Intense Laser Science, Shanghai 201800, China

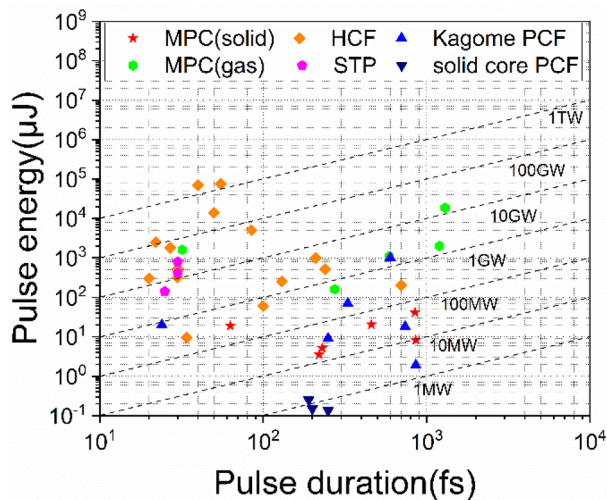


**Fig. 1** Overview of the input laser pulse parameter of different devices based on SPM effect

oscillator. The Gas-filled Kagome PCF can transmit laser pulses with the peak power ranging from megawatts to several gigawatts since the self-focusing threshold of noble gases is about three orders of magnitude lower than that of glass. Nevertheless, the Kagome PCF is sensitive to the beam pointing fluctuations of the input laser, because its core diameter is generally less than 100  $\mu\text{m}$ . The HCF can be implemented to broaden the spectrum of the high peak power laser pulse ( $\sim 100$  MW-TW) with a transmission of only  $\sim 50\%$ , and meanwhile it has poor long-term stability and bulky configurations. The STP can also applied in the high peak power laser systems, such as the kilohertz Ti: Sapphire amplifier. However, the output beam profile normally has a ring structure, and only the central part can be used in the experiments.

The above limitations can be mitigated by using the Herriott-type MPC, which is composed of nonlinear mediums (solid or gas) and two concave mirrors. During laser pulse propagation through the MPC, a small amount of nonlinear phase could be accumulated by one pass through the nonlinear medium. After several round trips, the strong and efficient spectral broadening can be achieved. This device was first demonstrated by Jan Schulte et al. in 2016, and they compressed the pulse duration of an Yb: YAG Innoslab amplifier from 850 to 170 fs with a transmission of  $> 90\%$  [34]. The advantages of the MPC are as follows. First, the output laser pulses from the MPC show an excellent beam profile and spectral-spatial homogeneity since the single-pass nonlinear phase shift is smaller like  $0.1\pi$  [37]. Second, the MPC can be constructed to have an ample aperture to make the device insensitive to the fluctuation and beam quality of the coupled laser beam [34]. Thirdly, the design flexibility of the MPC is terrific. There is a specific Gaussian

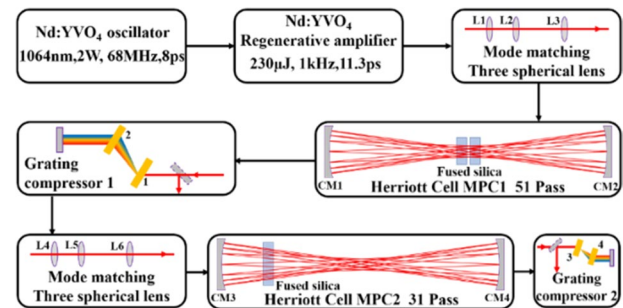


**Fig. 2** Experimental setup for nonlinear pulse compression a Nd: YVO<sub>4</sub> picosecond laser using two stages MPC, CM1-CM4: concave mirrors

eigenmode inside the MPC when the distance between the two concave mirrors is fixed. So, the per pass nonlinear phase is adjustable by changing the position of nonlinear elements along the axis of MPC. And the number of passes through the nonlinear medium can be changed by tuning the distance of the MPC mirrors with only a few millimeters. Therefore, the exact nonlinear phase could be accumulated by fine-tuning these parameters before the nonlinear loss occurs or the beam quality deteriorates significantly.

Benefiting from the above advantages, the MPC can efficiently broaden the spectrum of the laser pulses in a large peak power range. So far with the MPC devices, the peak power range of 10–302 MW in solids and 485 MW to 50 GW in noble gases have been reported [34–43]. For a pulse of 10 ps, its peak power will be tens of megawatt if the energy is several hundred microjoules. So, the MPC device with the solids as the nonlinear medium would be the best choice for our purpose. At present, the maximum incident pulse duration is 860 fs [36] and the optimal pulse compression ratio is 21 [42] based on the MPC with solids as the nonlinear mediums.

In this letter, we compress the pulse duration of a Nd: YVO<sub>4</sub> picosecond laser from 11.3 ps to 172 fs by a two-stage MPC with the fused-silica as the nonlinear medium, and the pulse duration is shortened by a factor of 66. The output pulse energy is 117  $\mu\text{J}$  with an incident energy of 230  $\mu\text{J}$ , corresponding to an overall efficiency of 51%. Our laser system is simple and compact. This is the first time that the MPC device has been employed to compress pulse around 10 ps. Moreover, this is the highest pulse compression ratio achieved in the MPC with solids nonlinear mediums.

## 2 Experimental setup

The experimental setup of the nonlinear temporal compression of a Nd: YVO<sub>4</sub> picosecond amplifier is depicted in Fig. 2. A Nd: YVO<sub>4</sub> based picosecond oscillator providing

2 W average power at the central wavelength of 1064 nm is used as the seed. The oscillator generates 8 ps pulses with a repetition rate of 68 MHz. The seed is directly injected into a 1 kHz Nd:YVO<sub>4</sub> regenerative amplifier without stretching the pulse width. The regenerative cavity is the same as that of 1 kHz amplifier in [44]. The pulse energy is amplified to 230  $\mu$ J and the pulse duration is stretched to 11.3 ps (Pulse-Check-50, A. P. E. GmbH) due to the gain narrowing effect, as shown in Fig. 3a. The spectrum of the amplified pulse has a bandwidth of 0.26 nm (FWHM) (OSA, YOKOGAWA AQ6370C), as shown in Fig. 3b, which supports the Fourier transform-limited (FTL) pulse duration of 5.9 ps. The mode matching of the picosecond laser to the first stage MPC is achieved using three spherical lenses (L1, L2, L3). The pulse duration will be broadened by the dispersion of the Kerr-mediums while the spectral broadening occurred. This will bring down the peak power of the input pulses and weakening the spectral broadening performance. Luckily, the pulse temporal broadening is negligible in our MPC device since overall silica length is much less than the dispersion length, which means it is unnecessary to compensate the material dispersion of Kerr-mediums by customized chirped concave

mirrors. So, easily available and affordable concave mirrors CM1-CM2 (CM508-150-E03, Thorlabs) are employed as MPC mirrors. The diameter and radius of curvature of CM1-CM2 is 50.8 mm and 300 mm, respectively. The distance between the CM1 and CM2 is 500 mm, and the beam diameter of the Gaussian eigenmode inside the MPC1 is  $2\omega_1=0.95$  mm and  $2\omega_0=0.39$  mm on the surfaces of concave mirrors and in the middle of the MPC1, respectively. Two 10 mm thick fused-silica with 50.8 mm diameter are placed in the middle of the MPC1 as the nonlinear medium, each end faces of which are coated with antireflection in the range of 1028–1064 nm. The Kerr-lens with a focal length 309 mm changes the beam diameter to  $2\omega_1=0.82$  mm and  $2\omega_0=0.43$  mm, respectively. The picosecond pulse coupling into and from the MPC is realized with two 6 mm diameter plane mirrors. The laser is aligned to pass through 26 roundtrips inside the MPC1, corresponding to 51 times passes through the fused-silica, and the total optical path in the fused silica and in air is 1.02 m and 24.48 m, respectively. A pair of 1000 line/mm transmission gratings is used for removing the positive chirp introduced by the SPM effect and the fused-silica material dispersion. After grating compressor1, the mode matching of the beam to the second stage MPC is also realized with three spherical lenses (L4, L5, L6). The MPC2 consists of mirrors (CM3, CM4) with the same parameters as those in MPC1 because the dispersion of nonlinear medium also has a weak effect on the accumulation of nonlinear phases. The distance between two concave mirrors is chosen to be 550 mm for a larger beam size in the concave mirrors to avoid the damage of the coating. The beam diameter is 0.335 mm at the cavity center, and 1.16 mm on the concave mirrors. A 10 mm thick fused-silica is placed 8.5 cm away from the CM3, and the beam diameter in the center of that is 0.82 mm, which changes to 0.88 mm due to the Kerr-lens effect. During a complete pass through the MPC2, the laser pulse is reflected 30 times on CM3 and CM4, plus reflection on the plane mirrors with 6 mm diameter for coupling in and out, corresponding to 31 times passes through the fused-silica. The optical path in the second stage MPC is 0.31 m and 16.74 m in the fused silica and air, respectively. Finally, a pair of gratings with 600 lines/mm groove are inserted into the system for compensating the positive chirp.

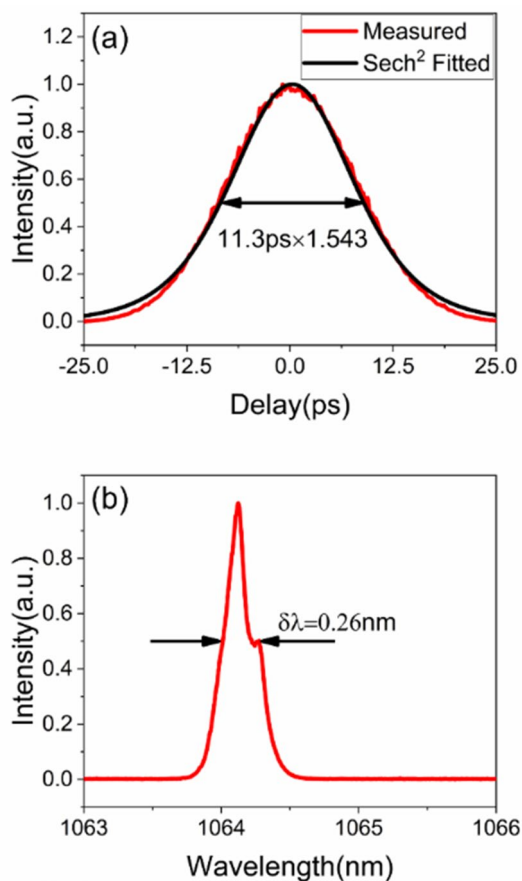


**Fig. 3** Intensity autocorrelation trace (a) and spectrum (b) of the Nd:YVO<sub>4</sub> regenerative amplifier

### 3 Experimental results

We use a half-wave plate and a thin-film polarizer to adjust the input pulse energy, the output pulse energy of both two stages MPC increases linearly with the increasing of the input pulse energy, which implies that no nonlinear loss occurred. The maximum output pulse energy of the first stage MPC is 180  $\mu$ J when the input pulse energy is 230  $\mu$ J,

which yields a transmission efficiency of 78%. The loss mainly stems from the 204 times reflection on the fused-silica end faces and 50 times reflection on the concave mirrors. The nonlinear phase of each passing through the nonlinear elements decreases on account of the reducing pulse energy in MPC device. The average nonlinear phase of per pass is calculated to be  $0.1\pi$ , so the total accumulated nonlinear phase in MPC1 is estimated to be  $5.1\pi$ . The spectrum after MPC1 is broadened from 0.26 to 2.5 nm (taken at half the intensity of the outer spectral maxima), which supports the FTL pulse duration of 1.04 ps, as shown in Fig. 4a. The number and intensity distribution of the peaks of the experimental spectrum is different from the theoretical values because the initial incident laser pulses are not FTL. Since the chirped mirrors or GTI mirrors cannot provide the required amount of GDD, which is at the magnitude of  $10^6$  fs<sup>2</sup>, so a pair of transmission gratings are used to compress the chirped pulses ones at the cost of introducing additional third-order-dispersion (TOD). The laser pulses are incident on the 1000 line/mm gratings at a Littrow angle of  $32.1^\circ$  to obtain the highest diffraction efficiency. Grating2 is mounted

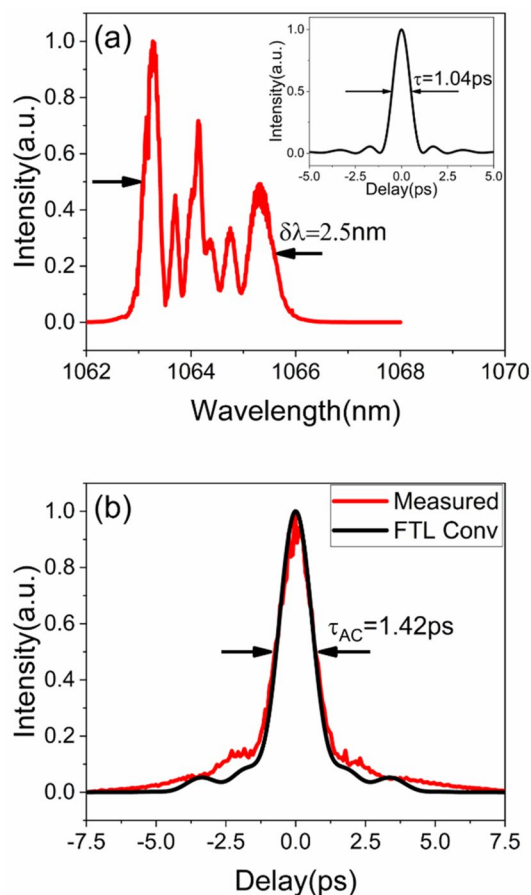


**Fig. 4** Characterization of the laser pulses from the first stage MPC. **a** broadened spectrum and FTL pulse; **b** measured autocorrelation trace and convolution of the FTL pulse

on a translation stage to adjust the GDD of compressor1. The shortest intensity autocorrelation trace after compressor1 is 1.42 ps when the distance between the grating pair is 385 mm, as shown in Fig. 4b. The GDD offered by the compressor1 is calculated to be  $-2.71 \times 10^6$  fs<sup>2</sup>. Assuming that the deconvolution factor of the compressed pulse is the same as the FTL (0.74), which yields an approximate compressed pulse of 1.05 ps. So, the laser pulse duration is shortened by a factor of 11. The remaining pulse energy is 157  $\mu$ J after compression, corresponding to a compression efficiency of 87.5%. By integrating the autocorrelation trace we estimate that 76% of the energy is concentrated in the main peak, so the peak power of the pulse improved by a factor of 5.6 is achieved.

The energy of the pulses coupled into the second stage MPC after passing through the three mode matching lenses (L4, L5, L6) is 152  $\mu$ J. And the output pulse energy is 140  $\mu$ J, corresponding to the transmission of 92%. The transmission of the MPC2 is higher than MPC1, due to only one piece of the fused silica as the Kerr medium inside MPC2, as well as fewer round trips. The beam averaged nonlinear phase of each pass is calculated to be  $0.08\pi$ , which contributes to a total nonlinear phase of  $2.5\pi$ . After 31 passes, a spectrum bandwidth of 18.06 nm (taken at half the intensity of the outer spectral maxima) is achieved, which supports the FTL pulse duration of 164 fs, as shown in Fig. 5a. As for the distribution of the spectrum intensity, both sides are lower than the middle parts, this is the same phenomenon as [35]. This likely stems from side pulses of the laser pulse output by MPC1. A pair of 600 line/mm transmission gratings is used to remove the positive chirp of the pulse introduced by SPM effect in the MPC2. The laser is also incident on the gratings at a Littrow angle of  $18.6^\circ$  for the highest diffraction efficiency. A compressed autocorrelation width of 229 fs is obtained when the distance of the two gratings is 17 mm, as shown in Fig. 5b. The GDD generated by the grating compressor2 is  $-3 \times 10^4$  fs<sup>2</sup>. Assuming that the deconvolution factor of the pulse after compressor2 is the same as the FTL (0.75), the resulting compressed pulse duration is about 172 fs. The pulse duration is shortened by a factor of 6. The pulse energy is 117  $\mu$ J after compression, which yields a compression efficiency of 83.6%. Based on the autocorrelation trace, we estimated that a fraction of 45% pulse energy is in the main pulse. And the energy outside the main peak may be caused by the high-order dispersion introduced by the grating compressor.

The laser beam quality ( $M^2$ ) output from the grating compressor2 in the horizontal and vertical directions are 1.36 and 1.45 (Spiricon,  $M^2$ -200 s), as shown in Fig. 6b. The spatial profile of the laser beams is well enough, as shown in the inset of the Fig. 6b. In addition, the laser beam profile is slightly deteriorated compared with the Nd: YVO<sub>4</sub> picosecond regenerative amplifier, the  $M^2$  value of which is

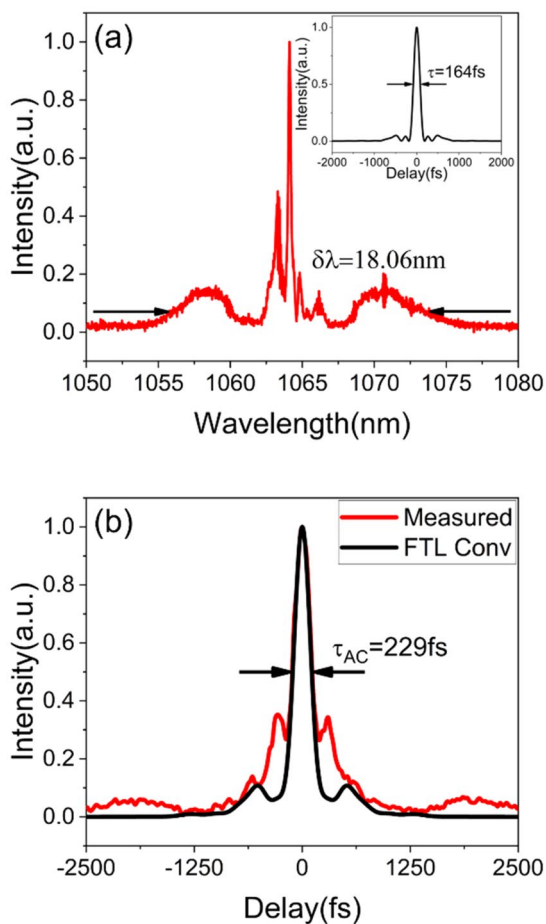


**Fig. 5** Characterization of the pulses from the second stage MPC. **a** broadened spectrum and FTL pulse; **b** measured autocorrelation trace and convolution of the FTL pulse

1.22 × 1.24, as shown in Fig. 6a. This result may be attributed to the imperfect concave mirrors shape and the Kerr lens effect [38].

### 4 Summary

In conclusion, we combined the MPC technology with the 10 ps level ultrafast lasers to generate 0.1 mJ level femtosecond pulses without CPA. Pulse compression of a Nd:YVO<sub>4</sub> picosecond amplifier from 11.3 ps to 172 fs at 230 μJ pulse energy is experimentally achieved by means of nonlinear spectral broadening in the MPC with an efficiency of 51%. Higher compression efficiency is expected if higher transmittance fused-silica adopted as nonlinear medium and chirped mirrors applied to remove the positive chirp after the MPC2. In the future, cost-efficient high average power femtosecond laser can be generated by a combination of high average power Nd-doped picosecond laser [45, 46] and the

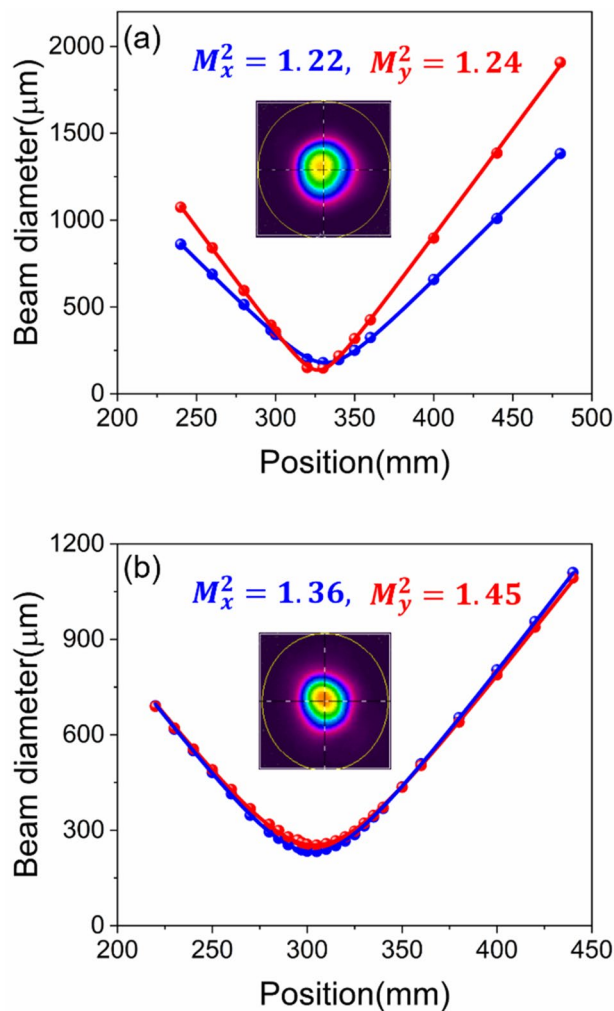


**Fig. 6** Beam quality of the regenerative amplifier (a) and MPC2 (b)

MPC technique. Such a laser source has potential in many different applications, like industrial micromachining and optical parametric amplification.

**Funding** National Natural Science Foundation of China (91850209, 11774410, 61575217); Key-Area Research and Development Program of Guangdong Province (2018B090904003); Strategic Priority Research Program of CAS (XDB16030200).

### References

1. S.A. Ashforth, R.N. Oosterbeek, O.L.C. Bodley, C. Mohr, C. Aguergaray, M.C. Simpson, *Lasers Med. Sci.* **35**, 1263 (2020)
2. G.D. Zhang, G.H. Cheng, *Appl. Optics* **54**, 8957 (2015)
3. B. Le Drogoff, F. Vidal, S. Laville, M. Chaker, T. Johnston, O. Barthelemy, J. Margot, M. Sabsabi, *Appl. Optics* **44**, 278 (2005)
4. I.B. Mukhin, M.R. Volkov, I.A. Vikulov, E.A. Perevezentsev, O.V. Palashov, *Quantum Electron.* **50**, 321 (2020)

5. J. Du, J. Harra, M. Virkki, J.M. Makela, Y.X. Leng, M. Kauranen, T. Kobayashi, *Sci. Rep.* **6**, 9 (2016)
6. M. Liebel, C. Schneidermann, T. Wende, P. Kukura, *J. Phys. Chem. A* **119**, 9506 (2015)
7. A.L. Calendron, H. Cankaya, F.X. Kartner, *Opt. Express* **22**, 24752 (2014)
8. A. Pugzlys, G. Andriukaitis, A. Baltuska, L. Su, J. Xu, H. Li, R. Li, W.J. Lai, P.B. Phua, A. Marcinkevicius, M.E. Fermann, L. Giniunas, R. Danielius, S. Alisauskas, *Opt. Lett.* **34**, 2075 (2009)
9. S. Ricaud, F. Druon, D.N. Papadopoulos, P. Camy, J.L. Doualan, R. Moncorge, M. Delaigue, Y. Zaouter, A. Courjaud, P. Georges, E. Mottay, *Opt. Lett.* **35**, 2415 (2010)
10. Z.G. Peng, M. Chen, C. Yang, L. Chang, G. Li, *Jpn. J. Appl. Phys.* **54**, 3 (2015)
11. Z.A. Bai, Z.W. Fan, Z.X. Bai, F.Q. Lian, Z.J. Kang, W.R. Lin, *Appl. Sci.-Basel* **5**, 359 (2015)
12. L.P. Ramirez, D.N. Papadopoulos, A. Pellegrina, P. Georges, F. Druon, P. Monot, A. Ricci, A. Jullien, X. Chen, J.P. Rousseau, R. Lopez-Martens, *Opt. Express* **19**, 93 (2011)
13. A. Jullien, L. Canova, O. Albert, D. Boschetto, L. Antonucci, Y.H. Cha, J.P. Rousseau, P. Chaudet, G. Cheriaux, J. Etchepare, S. Kourtev, N. Minkovski, S.M. Saliel, *Appl. Phys. B-Lasers Opt.* **87**, 595 (2007)
14. H. Fattahi, H. Wang, A. Alismail, G. Arisholm, V. Pervak, A.M. Azzeer, F. Krausz, *Opt. Express* **24**, 24337 (2016)
15. M. Seidel, J. Brons, G. Arisholm, K. Fritsch, V. Pervak, O. Pronin, *Sci. Rep.* **7**, 8 (2017)
16. W. Liu, C. Li, Z.G. Zhang, F.X. Kartner, G.Q. Chang, *Opt. Express* **24**, 15328 (2016)
17. W. Liu, S.H. Chia, H.Y. Chung, R. Greinert, F.X. Kartner, G.Q. Chang, *Opt. Express* **25**, 6822 (2017)
18. F.Z. Niu, J.Y. Li, W. Yang, Z.G. Zhang, A.M. Wang, *IEEE Photonics Technol. Lett.* **30**, 1479 (2018)
19. S. Hadrich, M. Krebs, A. Hoffmann, A. Klenke, J. Rothhardt, J. Limpert, A. Tunnermann, *Light-Sci. Appl.* **4**, 6 (2015)
20. F. Emaury, C.J. Saraceno, B. Debord, D. Ghosh, A. Diebold, F. Gerome, T. Sudmeyer, F. Benabid, U. Keller, *Opt. Lett.* **39**, 6843 (2014)
21. F. Guichard, A. Giree, Y. Zaouter, M. Hanna, G. Machinet, B. Debord, F. Gerome, P. Dupriez, F. Druon, C. Honninger, E. Mottay, F. Benabid, P. Georges, *Opt. Express* **23**, 7416 (2015)
22. F. Emaury, C.F. Dutin, C.J. Saraceno, M. Trant, O.H. Heckl, Y.Y. Wang, C. Schriber, F. Gerome, T. Sudmeyer, F. Benabid, U. Keller, *Opt. Express* **21**, 4986 (2013)
23. B. Debord, M. Alharbi, L. Vincetti, A. Husakou, C. Fourcade-Dutin, C. Hoenninger, E. Mottay, F. Gerome, F. Benabid, *Opt. Express* **22**, 10735 (2014)
24. B.H. Chen, M. Kretschmar, D. Ehberger, A. Blumenstein, P. Simon, P. Baum, T. Nagy, *Opt. Express* **26**, 3861 (2018)
25. M. Nisoli, S. DeSilvestri, O. Svelto, *Appl. Phys. Lett.* **68**, 2793 (1996)
26. S. Bohman, A. Suda, T. Kanai, S. Yamaguchi, K. Midorikawa, *Opt. Lett.* **35**, 1887 (2010)
27. X.W. Chen, A. Jullien, A. Malvache, L. Canova, A. Borot, A. Trisorio, C.G. Durfee, R. Lopez-Martens, *Opt. Lett.* **34**, 1588 (2009)
28. C.F. Dutin, A. Dubrouil, S. Petit, E. Mevel, E. Constant, D. Descamps, *Opt. Lett.* **35**, 253 (2010)
29. O. Hort, A. Dubrouil, A. Cabasse, S. Petit, E. Mevel, D. Descamps, E. Constant, *J. Opt. Soc. Am. B-Opt. Phys.* **32**, 1055 (2015)
30. J. Rothhardt, S. Hadrich, H. Carstens, N. Herrick, S. Demmler, J. Limpert, A. Tunnermann, *Opt. Lett.* **36**, 4605 (2011)
31. C.H. Lu, Y.J. Tsou, H.Y. Chen, B.H. Chen, Y.C. Cheng, S.D. Yang, M.C. Chen, C.C. Hsu, A.H. Kung, *Optica* **1**, 400 (2014)
32. P. He, Y.Y. Liu, K. Zhao, H. Teng, X.K. He, P. Huang, H.D. Huang, S.Y. Zhong, Y.J. Jiang, S.B. Fang, X. Hou, Z.Y. Wei, *Opt. Lett.* **42**, 474 (2017)
33. M. Seo, K. Tsendsuren, S. Mitra, M. Kling, D. Kim, *Opt. Lett.* **45**, 367 (2020)
34. J. Schulte, T. Sartorius, J. Weitenberg, A. Vernaleken, P. Russbuehldt, *Opt. Lett.* **41**, 4511 (2016)
35. J. Weitenberg, T. Saule, J. Schulte, P. Russbuehldt, *IEEE J. Quantum Electron.* **53**, 4 (2017)
36. J. Weitenberg, A. Vernaleken, J. Schulte, A. Ozawa, T. Sartorius, V. Pervak, H.D. Hoffmann, T. Udem, P. Russbuehldt, T.W. Hansch, *Opt. Express* **25**, 20502 (2017)
37. K. Fritsch, M. Poetzlberger, V. Pervak, J. Brons, O. Pronin, *Opt. Lett.* **43**, 4643 (2018)
38. M. Kaumanns, V. Pervak, D. Kormin, V. Leshchenko, A. Kessel, M. Ueffing, Y. Chen, T. Nubbemeyer, *Opt. Lett.* **43**, 5877 (2018)
39. L. Lavenu, M. Natile, F. Guichard, Y. Zaouter, X. Delen, M. Hanna, E. Mottay, P. Georges, *Opt. Lett.* **43**, 2252 (2018)
40. P. Russbuehldt, J. Weitenberg, J. Schulte, R. Meyer, C. Meinhardt, H.D. Hoffmann, R. Poprawe, *Opt. Lett.* **44**, 5222 (2019)
41. C.L. Tsai, F. Meyer, A. Omar, Y.C. Wang, A.Y. Liang, C.H. Lu, M. Hoffmann, S.D. Yang, C.J. Saraceno, *Opt. Lett.* **44**, 4115 (2019)
42. E. Vicentini, Y.C. Wang, D. Gatti, A. Gambetta, P. Laporta, G. Galzerano, K. Curtis, K. McEwan, C.R. Howle, N. Coluccelli, *Opt. Express* **28**, 4541 (2020)
43. P. Balla, A. Bin Wahid, I. Sytcevich, C. Guo, A.L. Viotti, L. Silletti, A. Cartella, S. Alisauskas, H. Tavakol, U. Grosse Wortmann, A. Schonberg, M. Seidel, A. Trabattoni, B. Manschwetus, T. Lang, F. Calegari, A. Couairon, A. L'Huillier, C.L. Arnold, I. Hartl, C.M. Heyl, *Opt. Lett.* **45**, 2572 (2020)
44. J.X. Liu, W. Wang, Z.H. Wang, Z.G. Lv, Z.Y. Zhang, Z.Y. Wei, *Appl. Sci.-Basel* **5**, 1590 (2015)
45. X.S. Liu, W.Z. Jia, Y.H. Song, S. Yang, S. Liu, Y.Q. Liu, A.R. Yan, Z.Y. Wang, *Opt. Express* **28**, 8016 (2020)
46. K. Michailovas, V. Srnilgevičius, A. Michailovas, *Lith. J. Phys.* **54**, 150 (2014)

**Publisher's Note** Springer Nature remains neutral with regard to jurisdictional claims in published maps and institutional affiliations.